19th WORLD CONFERENCE OF THE ASSOCIATED RESEARCH CENTRES FOR THE URBAN UNDERGROUND SPACE
Belgrade, Serbia, November 4-7, 2025.

ACUUS BELGRADE 2025

Paper No: 7.5.219
DOI: 10.46793/ACUUS2025.7.5.219

COMPRESSED AIR ENERGY STORAGE (CAES) SYSTEM IN ARTIFICIAL UNDERGROUND CAVERNS WITHIN ROCK SALT FORMATION OF MONOLITHI, IOANNINA, GREECE.

Konstantinos Bampousis[1, 2], Ioannis Vlachogiannis[1, 2], Andreas Benardos[1]

Abstract: Compressed Air Energy Storage (CAES) is emerging as a strategic solution to address the increasing need for scalable, long-duration energy storage in systems with high renewable penetration. As Greece transitions toward decarbonized electricity networks, the Monolithi site in Ioannina offers a unique opportunity to develop the country's first underground CAES system using naturally sealed salt formations. This study evaluates the feasibility, design optimization, and long-term geomechanical stability of artificial spherical storage caverns within the halite deposit, which lies at a depth of approximately 150 m and exhibits high cohesion and low permeability.

The geological and geotechnical assessment was conducted using historical data from Hellenic Survey of Geology & Mineral Exploration (HSGME), followed by 2D and 3D numerical analyses to assess the optimal design of the complex and to evaluate its performance in the construction and operation phase, in terms of stability. This optimization in the design started from a simplistic layout of 2 main caverns and finally progressed in the suggestion of a 3-cavern layout that allowed for an increased capacity, ensuring the feasibility of the project. At the same time the analysis verified the stability of the cavern structures at all construction and operating conditions, with limited plastic zone development and displacements. More particularly, the 3D numerical analyses confirmed the optimal caverns' spatial configuration and insights were attained for all important effects, such as surface uplift and stress redistribution near cavern boundaries, validating the benefits of internal pressurization. The system remained structurally stable with all strength factors exceeding safety thresholds - even under a full cyclic pressure range (0-6-0 MPa).

Thermodynamic calculations estimate an energy potential of 150 MWh per cycle, translating to up to 30 GWh/year under modern round-trip efficiency assumptions (70%) and 300 annual cycles. The initial CAPEX is estimated between 19,5–29,3 million EUR, indicating that the Monolithi CAES system could represent a cost-effective, spatially flexible alternative to pumped hydro storage. This research demonstrates the critical role of 3D numerical modeling in design validation and highlights the strategic importance of such infrastructure in supporting Greece's renewable integration and compliance with EU decarbonization objectives.

Keywords: CAES, Salt Caverns, 3D Numerical Modeling, Energy Storage, Greece Energy Transition

1. INTRODUCTION

The global shift toward renewable energy has accelerated the need for robust, long-duration energy storage systems capable of balancing intermittent generation and ensuring grid stability. Technologies such as Compressed Air Energy Storage (CAES) are gaining renewed attention due to their scalability, longevity, and compatibility with underground geological formations. In contrast to lithium-ion batteries or pumped hydroelectric storage, CAES systems offer a cost-effective solution particularly well-suited for regions with suitable subsurface conditions, such as halite (rock salt) formations.

[1] National Technical University of Athens, School of Mining & Metallurgical Engineering, Athens, GR15780, Greece
[2] Geomine J&K, Athens, GR14451, Greece

In the European Union, and particularly in Greece, the integration of wind and solar power has led to increasing instances of overgeneration and curtailment. These developments highlight an urgent need for storage technologies capable of absorbing excess energy during off-peak periods and releasing it when demand surges. Recognizing this, the European Commission has identified underground storage—including CAES—as a key enabler of the EU's climate-neutral energy system objective by 2050 [European Parliament, 2020].

Salt formations, with their high sealing capacity, low permeability, and favorable ductile behavior under stress, offer ideal conditions for CAES cavern development. In northwestern Greece, the Monolithi area presents a notable geological opportunity: a thick halite dome, previously studied by the Hellenic Survey of Geology & Mineral Exploration (HSGME) [21] [14], that may support the development of the country's first underground energy storage system of this type.

This paper investigates the design and feasibility of an underground CAES system that can be developed in salt caverns at the Monolithi salt deposit. Emphasis is given on the design with the use of advanced 3D finite element modeling (FEM), which enables a more comprehensive assessment of stress interactions, deformation behavior, and operational safety than conventional two-dimensional approaches. The objective is to evaluate whether the proposed cavern design can meet the structural and functional criteria required for safe and efficient operation, while also establishing a replicable model for Greece's energy transition aligned with European Union directives on renewable integration and energy resilience. Finally, an assessment of its feasibility is given, to bear in mind the required CAPEX expenditure as well as the benefits of the energy storage that can be offered by the underground CAES project.

2. THEORY AND NUMERICAL METHODS USED

This study assesses the feasibility and geomechanical stability of a Compressed Air Energy Storage (CAES) system in artificial underground salt caverns at the Monolithi site, Ioannina, Greece. The methodological approach combines geological modeling, empirical assumptions, and numerical analyses to evaluate the performance of the system under various operational pressures.

2.1. Geological and Geotechnical Data Collection

The geological characterization of the study area was based on historical data from the HSGME [15], including borehole logs, geological investigations, stratigraphy, and geophysical investigations conducted in the 1970s as shown in Figure 1. The predominant geological formation in the area is flysch, a low-permeability, mechanically heterogeneous sedimentary sequence that serves as the host rock. Within this formation, a dome-shaped halite body has intruded, forming a structurally confined salt deposit with an estimated thickness of approximately 90 m, suitable for underground storage applications. The salt deposit was modeled in 3D using Leapfrog Geo as illustrated in Figure 2, with inferred geometry calibrated through interpretation of available borehole information and structural data. Due to the lack of georeferenced borehole coordinates, spatial uncertainty was acknowledged and addressed through conservative modeling assumptions.

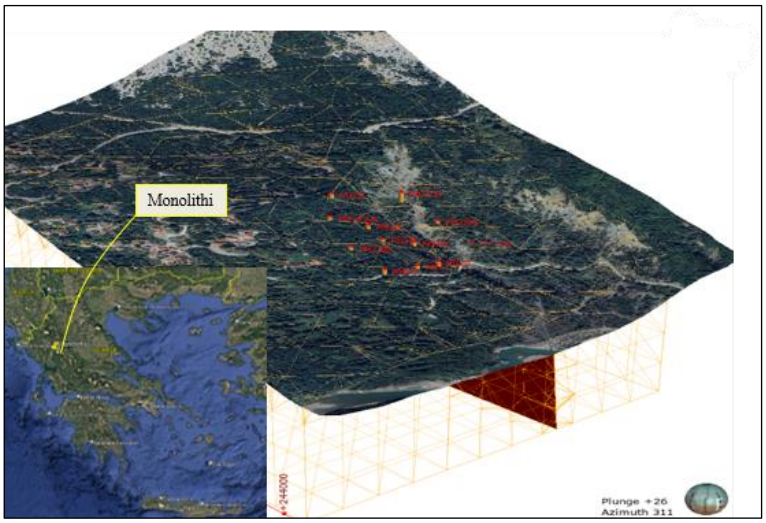

Figure 1. *Location of the Monolithi area and presentation of boreholes investigation layout (HSGME, 1996).*

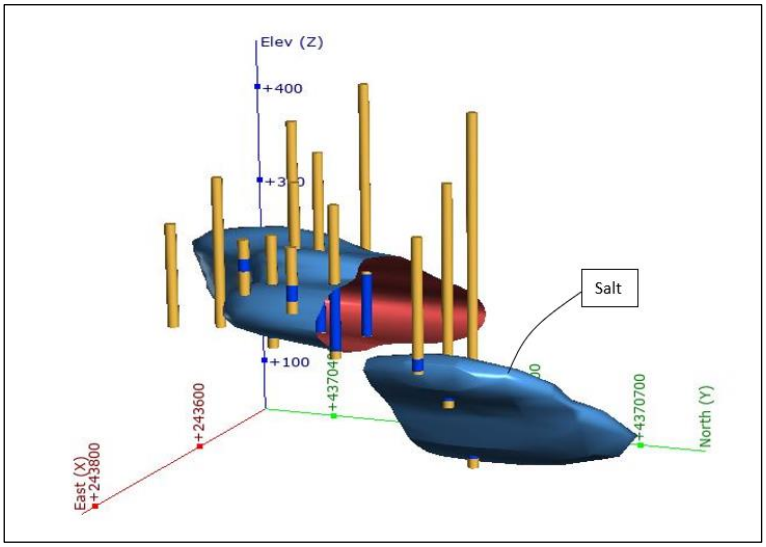

Figure 2. *Three-dimensional geological mapping of the rock salt deposit in the Monolithi area based on existing boreholes.*

2.2. Material Properties and Assumptions

Mechanical and physical properties of halite and surrounding flysch were derived from international literature and similar geological settings. For halite, typical values from the Klodawa, Poland [9] formation were adopted. Flysch properties were referenced from the Driskos tunnel study [22], as it closely resembles the local formation characteristics. In Table 1, these data are given as range values along with the finally selected design values for the project.

Table 1. *Characteristic Mechanical and Physical Properties of Rock Salt (Source: Kolano et al., 2024).*

Properties	**Range**	**Design value**
Poisson ratio, ν	0,04 – 0,49	0,35
Unit weight, γ (kN/m³)	28,4-22,5	21
Geological Strength Index, GSI	-	80*
Uniaxial compressive strength, σ_{ci} (MPa)	2,80 – 34,20	20
Young Modulus, E_i (GPa)	10 - 30	20
m_i	-	11
m_b	-	5.3
s	-	0,108
a	-	0,50
Deformation Modulus, E_{rm} (GPa)	0,4 – 4,9	3,5

*Intact rock salt formation with very good to good joint surface conditions.

Table 2. *Characteristic Mechanical and Physical Properties of Flysch (Source: Vlachopoulos et al., 2013).*

Properties	Design Value
Poisson ratio (v)	0,25
Unit weight, γ (kN/m³)	27 kN/m³
Geological Strength Index, GSI	31–40 (mean value: 35)
Uniaxial compressive strength, σ_{ci} (MPa)	26,25
Young modulus, Ei (GPa)	13.453
m_i	8
m_b	0,76
s	0,00073
a	0,52
Deformation Modulus, E_{rm} (GPa)	1,5

2.3. Geometry and model setup

The geometric layout of the underground compressed air energy storage (CAES) system evolved through successive 2D & 3D numerical analyses. In the initial phase, a 2D plane strain model was developed using Rocscience RS2 software. The authors acknowledge the inherent limitation of 2D FEA in accurately representing a pair of ideally spherical caverns, as it simulates the behavior of infinitely long tunnels. Nevertheless, this approach was intentionally selected as a starting point for the present investigation.

Moreover, spherical cavern geometry was selected due to its effectiveness attaining a favorable pressure distribution in the salt formation. Furthermore, this achieves a robust buffer zoning between the caverns and the boundaries of the salt formation. Several sizing and spacing scenarios were examined to prevent interaction between the caverns and ensure stable conditions. The 2D analysis results indicated the setup of two spherical caverns with a diameter of 45 m and 95 m distance center-to-center, satisfying the criteria for acceptable strength factor, limited displacements and plastic zone as shown in Figure 3.

To improve spatial setup and account for a much more realistic approach, a 3D finite element model (Figure 4) was developed using Rocscience RS3 software, validating the two cavern-configuration derived from the 2D analysis. Building on the results, a third spherical cavern with a diameter of 45 m was introduced to further optimize the use of the available salt volume and increase the capacity of the complex. The three caverns were arranged in an equilateral triangular pattern with 60° angular spacing and center-to-center distances reduced to 80 m. This arrangement was specifically chosen to evaluate the structural integrity and performance of the underground project, checking and evaluating potential interactions between the cavern structures.

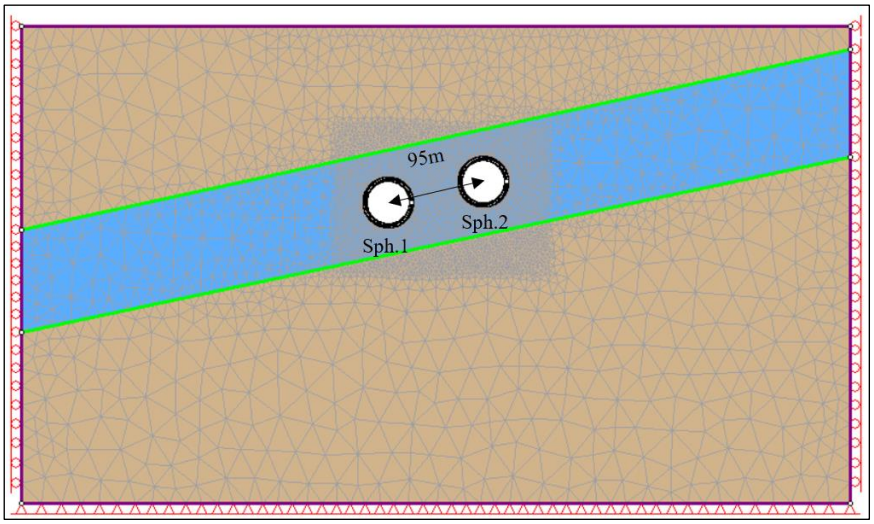

Figure 3. *2D model setup and generated mesh for FEA.*

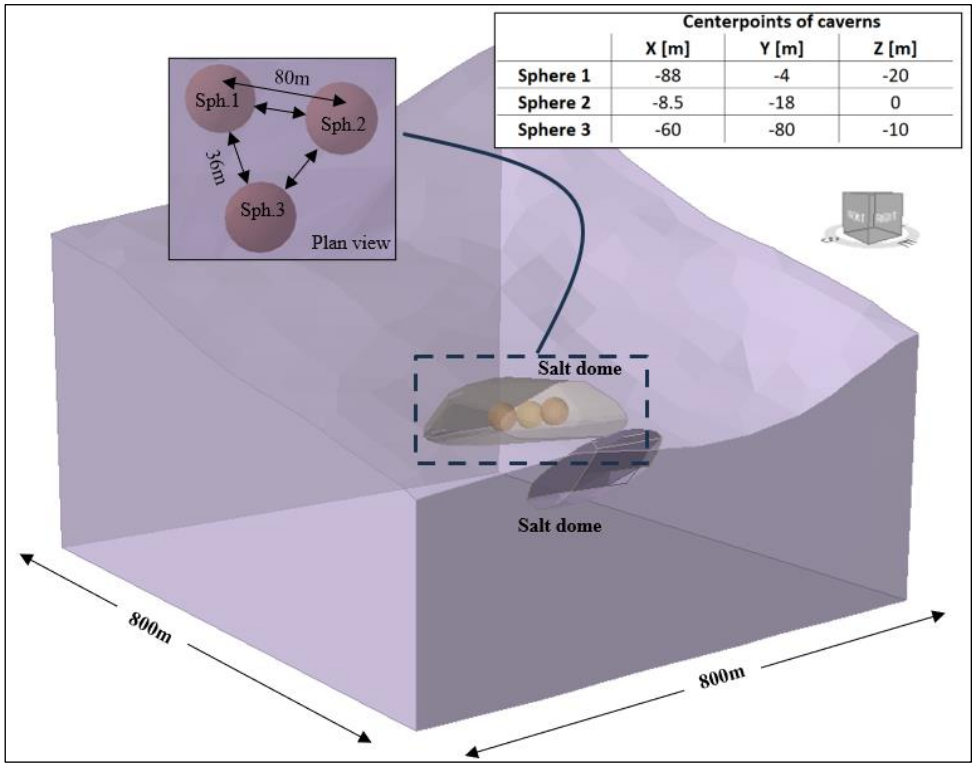

Figure 4. *3D model setup for FEA.*

In both 2D and 3D analysis, the gravity type stress condition was selected to simulate the in-situ field stress, with a horizontal to vertical stress ratio, k (σ_h/σ_v) set to 1. The material behavior was modeled as a least – perfect plastic, using the Generalized Hoek–Brown constitutive criterion.

The boundary conditions were defined such as that the base of the model was fully constrained in all directions, while the lateral boundaries were restricted only in the horizontal direction, allowing free vertical movement. In the 2D analysis a graded mesh composed of 3-noded triangular elements was employed, resulting in approximately 10.000 elements for accurate resolution of stress and displacement fields around the cavern boundaries, while a refinement area (200m x 150m) with a uniform 5m element length was applied to achieve more accurate and detailed results around the caverns. In the 3D analysis a graded mesh of 4-noded tetrahedral elements was applied, resulting in the generation of more than 400.000 elements (Figure 5).

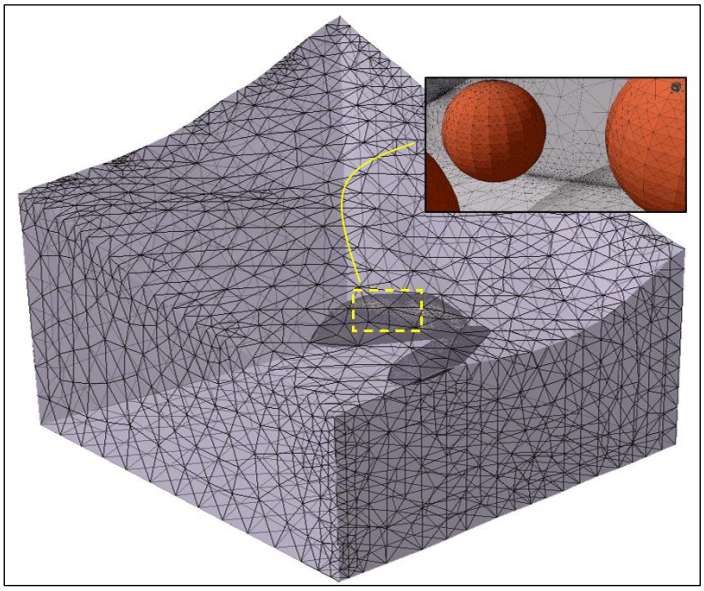

Figure 5. *Generated mesh for 3D FEA.*

The loading sequence applied in both 2D, and 3D numerical models was modelled to replicate a full operational cycle of a CAES system, including both charging (pressurization) and discharging (depressurization) phases. Initially, the caverns were simulated in an unpressurized state immediately following excavation, representing zero internal pressure. Subsequently, internal pressure was incrementally increased in steps of 0,8 MPa, up to a maximum operational pressure of 6,0 MPa. After reaching the peak pressure, the system was gradually unloaded following the same stepwise pattern—decreasing the internal pressure by 0,8 MPa per stage until it returned to 0 MPa. This symmetric pressure path allowed for the evaluation of the geomechanical response of the surrounding rock mass under cyclic loading-unloading, including stress redistribution, development of plastic zones, and potential residual deformations induced by the pressure reversals.

3. RESULTS

The results of the analysis are given hereinafter. The primary objective is to assess the geomechanical stability and performance of the proposed CAES cavern configurations under internal pressure and geostatic stress conditions. Key metrics evaluated include vertical displacements, strength factor (SF) distributions, and plastic zone development, with special emphasis on comparing the behavior observed in 2D versus 3D analyses. The following figures provide a detailed summary of the model geometries, material parameters, and results from each scenario, enabling a direct comparison of performance and recorded deformation specifics between the two modeling approaches.

3.1. 2D Results

The numerical analyses conducted in RS2 revealed limited vertical displacements. During the excavation phase (P = 0 MPa), the maximum surface settlement was recorded at -2 mm, while the vertical displacement at the crown of the cavity reached -10 mm (Figure 6). In the subsequent pressurization phase, 60 bar (P = 6,0 MPa), the displacements increased, as expected: surface rose to +11 mm, and vertical displacement at the crown reached +18 mm (Figure 7). Despite the increase, these values remain within stability thresholds and do not indicate any structural compromise. Overall, the 45 m diameter configuration exhibited predictable deformation behavior and maintained geometric integrity throughout the successive pressurization and de-pressurization process.

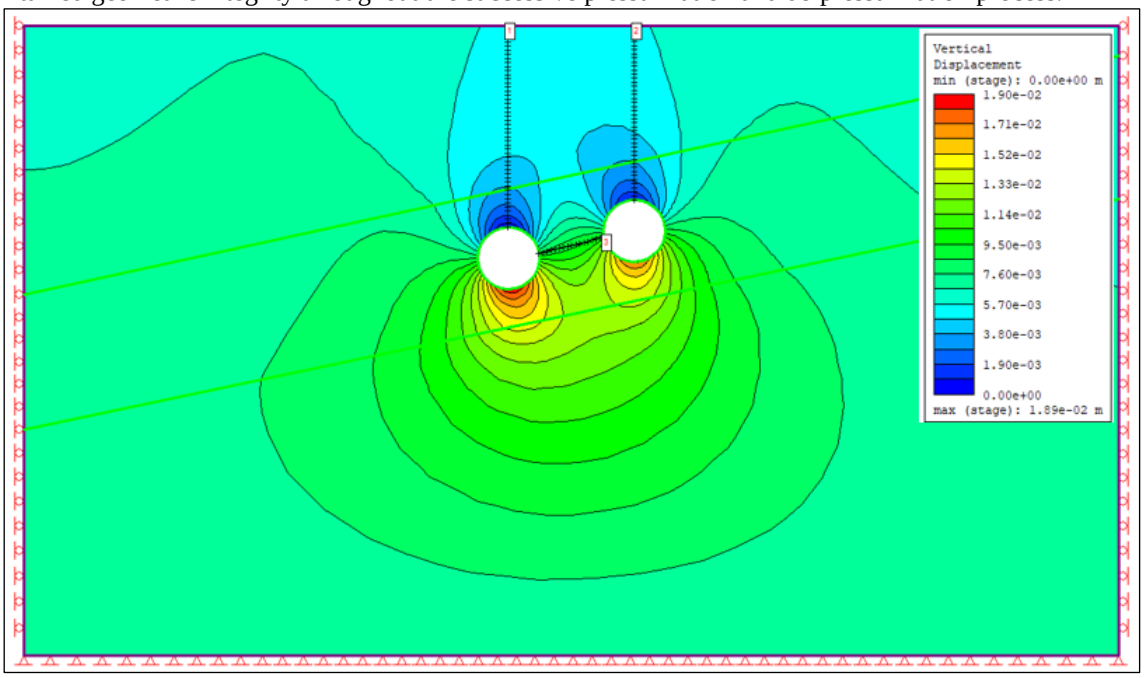

Figure 6. *Vertical displacement after the excavation in the 2D analysis.*

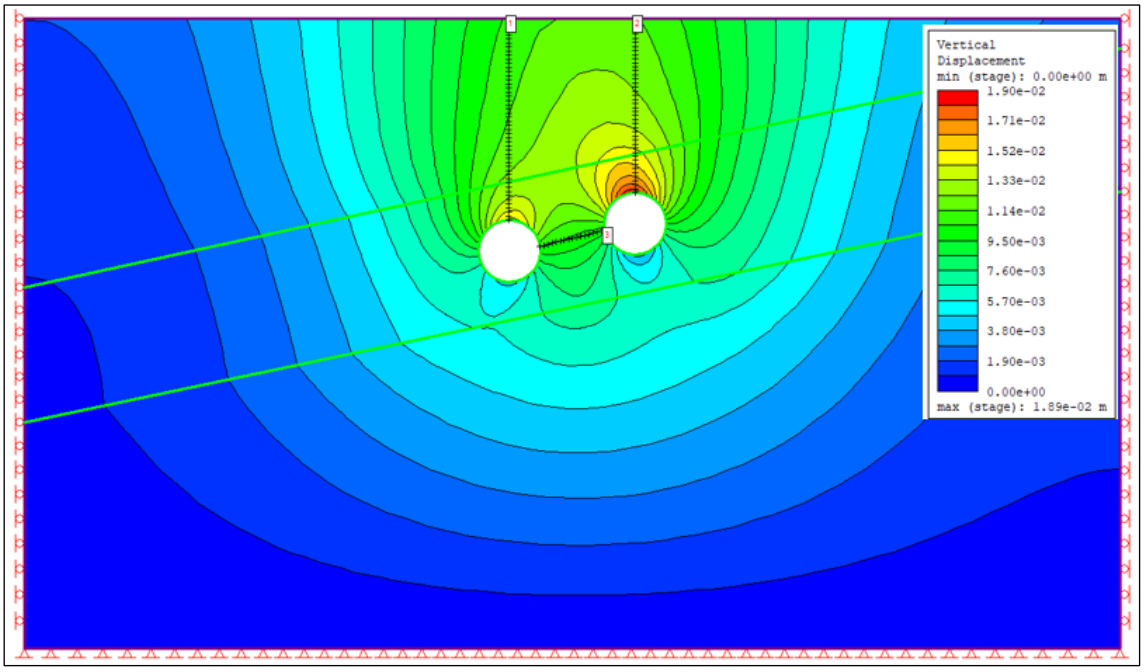

Figure 7. *Vertical displacement after applying 6Mpa internal pressure in the 2D analysis.*

As shown in the corresponding displacement graph (Figure 8), the transition from excavation to maximum pressurization results in a clear uplift pattern above the storage sphere. The plot highlights a reversal in the displacement field from negative (subsidence) to positive (heave) - with the maximum vertical uplift concentrated directly above the crown of sphere 2.

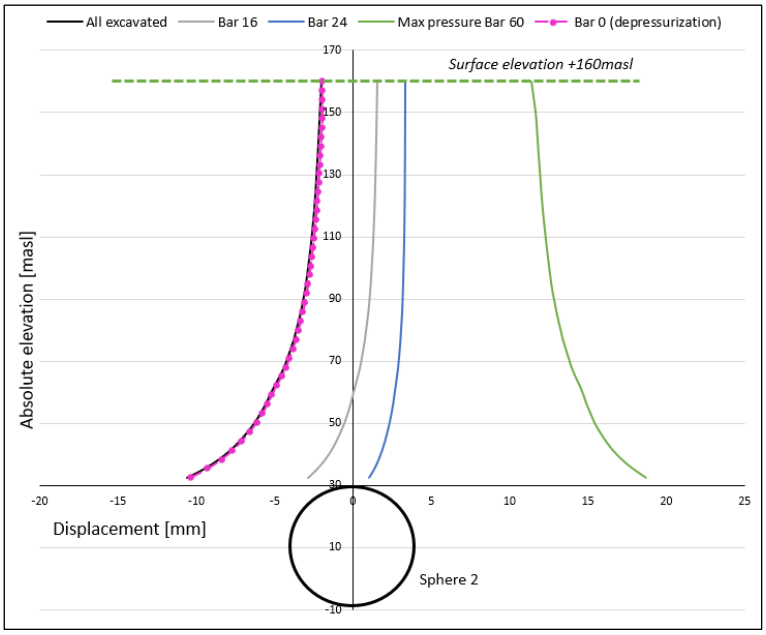

Figure 8. *Vertical displacement distribution above Sphere 2.*

The Strength Factor (SF) between the caverns remains above 1.0 (Figure 9) across all along pillar formed between the two caverns right after the excavation with a narrow plastic zone of 3,0m around the caverns. In Figure 10, the formed pillar consistently remains above stable limits, with the SF above 2.0 in low pressurized state and reaching approximately 4.1 under an internal pressure of 60 bar (6,0Mpa).

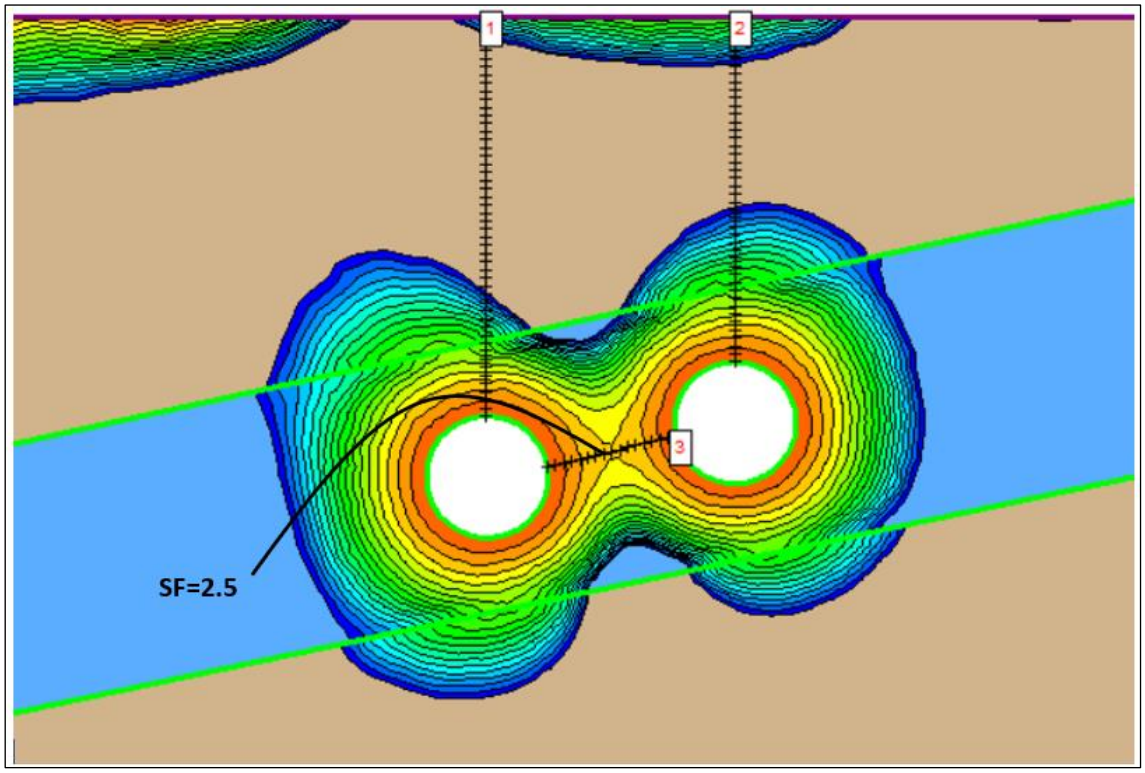

Figure 9. *Strength factor between caverns (stage: all caverns excavated).*

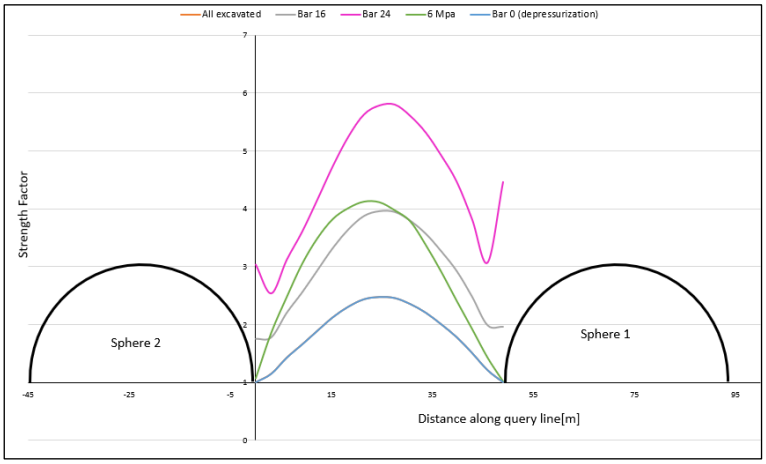

Figure 10. *Strength factor along the query line between the caverns.*

3.2. 3D Results

The vertical displacement as imposed on the surface area is given in Figure 11, with a contour interval of 1 mm. On the left, the surface deformation is shown after the full excavation of all caverns, where a localized settlement zone is observed directly above the caverns, with maximum vertical displacements reaching approximately −2 mm. In contrast, on the right, it highlights the effect of internal pressurization at 60 bars. The ground surface directly above the cavern experiences a small uplift, with peak vertical displacements reaching up to 7-8 mm. This behavior illustrates the interplay between excavation-induced subsidence and pressure-induced uplift phenomena. The analysis confirms that internal pressurization substantially mitigates surface settlement and can even result in net uplift—an effect that is crucial for maintaining the stability of surface infrastructure in CAES operations.

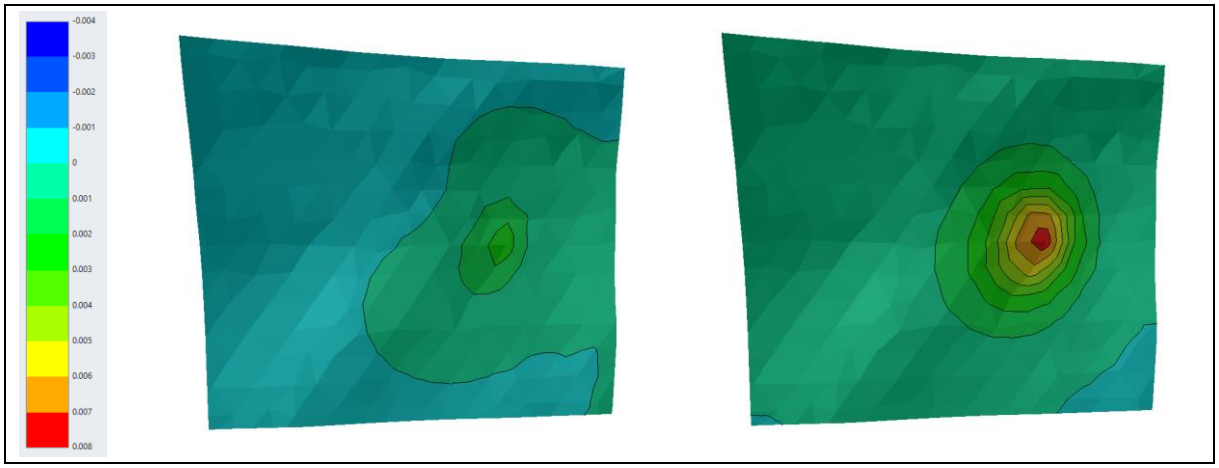

Figure 11. *Vertical displacement contours on surface with 1mm interval (left: after excavation; right: at operational phase with a max pressure of 60 bar (6 MPa)).*

Vertical displacements occurring directly above Sphere 2, from the cavern crest up to the ground surface at +125 masl, are presented in Figure 12 and Figure 13. The profile illustrates how the rock mass responds to excavation and internal pressurization. Following full excavation, the zone above the cavern undergoes measurable subsidence, with downward displacements reaching approximately 6mm near the cavern roof and gradually decreasing toward the surface. As internal pressure increases, this trend is reversed. At the maximum internal pressure of 60 bars, a distinct uplift develops in the same zone (green curve), with vertical displacements exceeding +24 mm at the cavern roof and remaining noticeable up, approximately +7 mm at the ground surface. This behavior highlights the sensitivity of the overburden to internal pressure changes and emphasizes the role of pressurization in controlling possible settlements above the underground storage caverns.

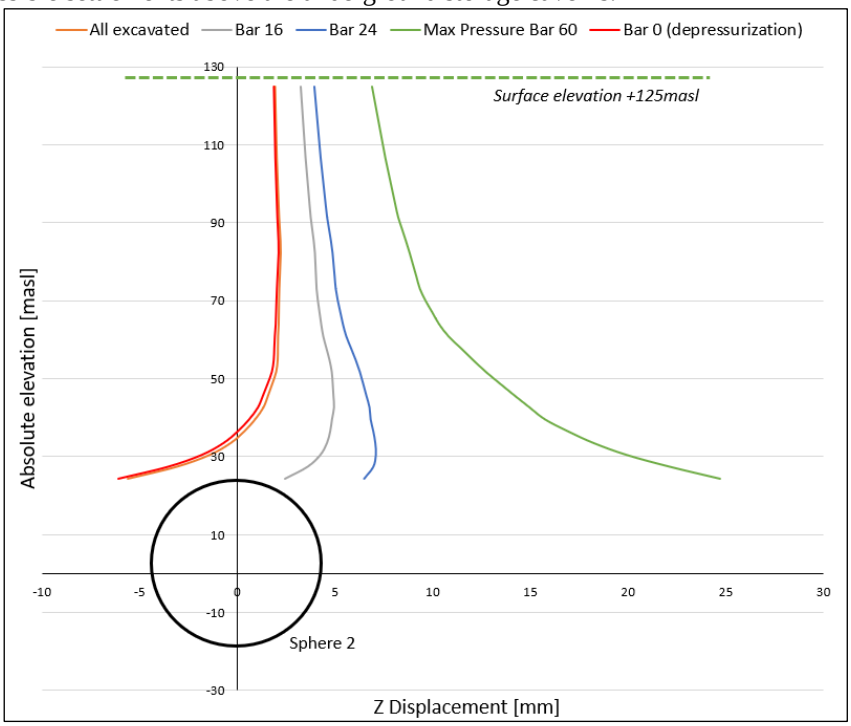

Figure 12. *Vertical displacement distribution above Sphere 1.*

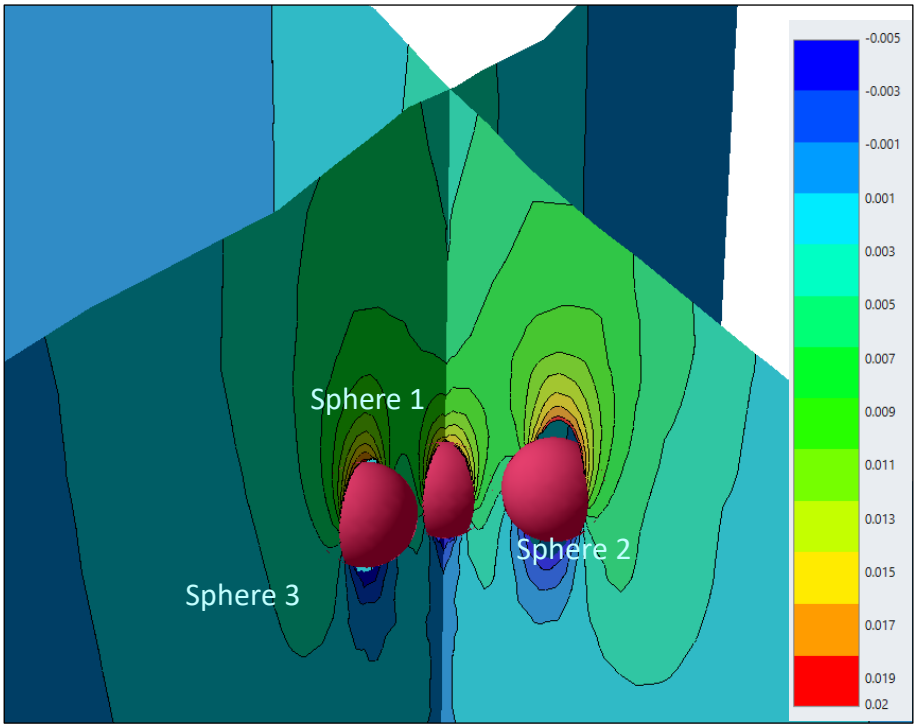

Figure 13. *Vertical displacements at the underground cavern complex (stage: max pressure, 60bar).*

The strength factor (SF) distribution in the region between the caverns after the full excavation stage is presented in Figure 16. The 3D contour plot reveals that the maximum SF values range from 2,5 to 2,7 (Figure 14).

An accompanying graph shown in Figure 15 illustrates how the strength factor (SF) varies along a horizontal line that passes through the rock pillar between caverns, starting at Sphere 3 and moving toward and between Spheres 1 and 2. It shows how excavation and different internal pressure levels affect the stability of the surrounding rock. Specifically, when all caverns are excavated without any internal pressure, the SF drops to a minimum of just above 1,0 immediately adjacent to Sphere 3, indicating the plastic zone formed around the underground opening. As the distance from the cavern increases and the line approaches the central region between the three spheres, i.e. within the core of the inter-cavern pillar, the SF rises reaching a maximum of approximately 4,5 (for stage: 24 bars). However, under the maximum internal pressure of 60 bars (6 MPa), a markedly different trend emerges: the SF elevates to values above 8 right next to the cavern wall because of internal pressure, and then gradually settles to uniform values of 3,3 along the central part of the pillar. This reversal of the typical SF gradient highlights the strong influence of high internal pressure in improving local stability around the openings. The mechanism behind the increase of the SF lies in the lateral forces imposed through the air pressure in the cavern that provides a significant σ_3 stress regime that increases the ultimate strength of the pillar between caverns.

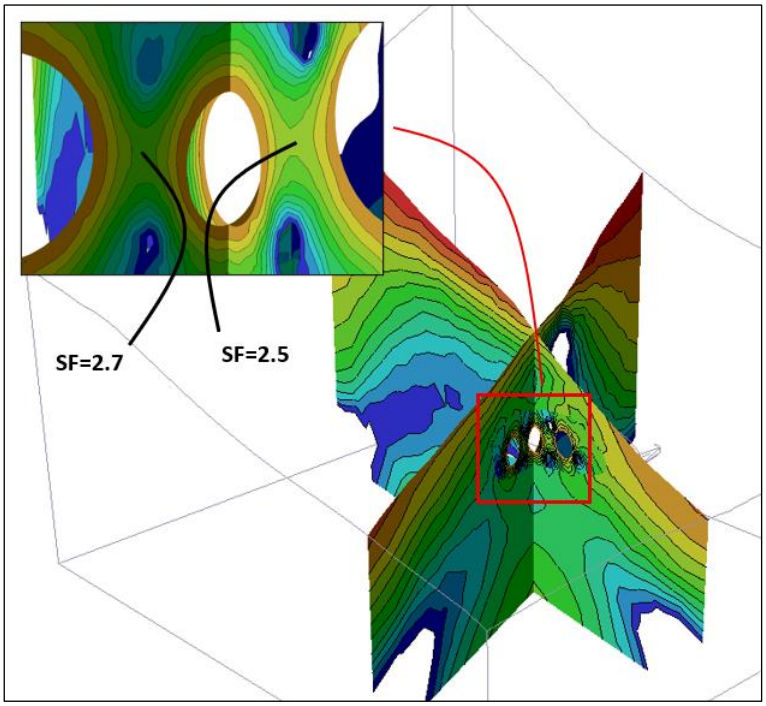

Figure 14. *Strength factor contours and values at regions between caverns (stage: all caverns excavated).*

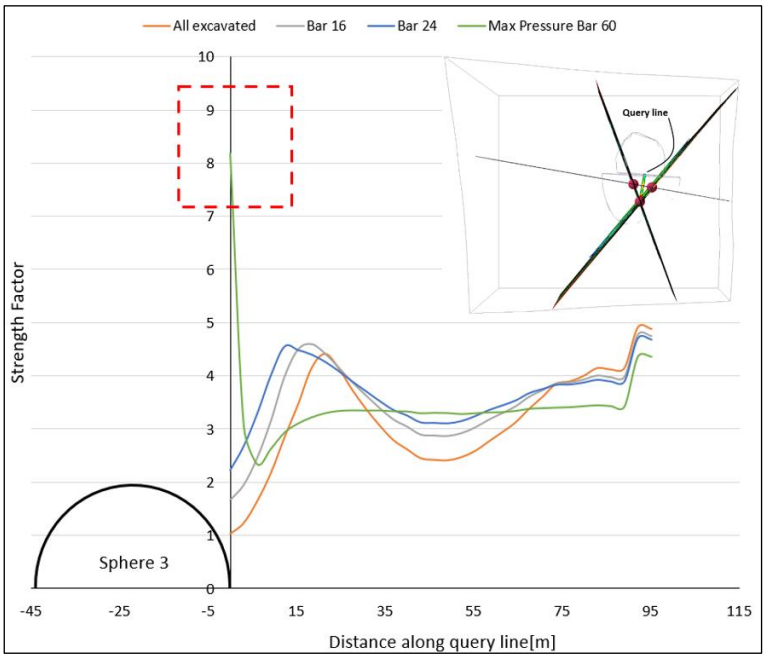

Figure 15. *Strength factor along query line extending through the enclosed pillar (surrounded by the three caverns).*

3.3. Thermodynamic Estimation of Recoverable Energy

The thermodynamic assessment of the theoretical energy output that can be recovered from the CAES scheme is crucial for the assessment of the overall feasibility of the storage project. The preliminary approach presented in this section is based on principal thermodynamic equations that describe the adiabatic expansion of an ideal gas:

$$W = \frac{nRT}{\gamma - 1}\left[1 - \left(\frac{P_i}{P_i}\right)^{\frac{\gamma-1}{\gamma}}\right] \tag{1}$$

Where:

- W: Total mechanical energy recovered (Joules)
- n: Number of moles of air in the reservoir
- R: Specific gas constant for air (287 J/kg·K)
- T: Absolute temperature (Kelvin)
- γ: Adiabatic expansion coefficient (γ = 1,4 for air)
- P_1, P_2: Initial and final pressure (Pa)

Each storage unit (cavern) is a sphere with a diameter of 45 m, resulting in an individual volume of:

$$V = \frac{4}{3}\pi R^3 = 47{,}713\, m^3$$

Other assumptions of the project are:

- Temperature: T = 300 K
- Initial pressure: $P_1 = 6{,}0 \cdot 10^6$ Pa
- Final pressure: $P_2 = 1{,}5 \cdot 10^6$ Pa
- Number of spheres: 3

The number of moles stored in each cavern is given by:

$$n = \frac{P_i \cdot V}{R \cdot T} \tag{2}$$

where V is the volume of the storage cavern. Finally, the conversion of the energy result from Joules to megawatt-hours is performed using:

$$E_{\mathrm{MWh}} = \frac{W}{3{,}6 \cdot 10^9} \tag{3}$$

Using Equation (2), the number of moles of air per cavern is:

$$n = \frac{6 \times 10^6 \cdot 47{,}713}{287 \cdot 300} \approx 3.324.943 \text{ mol}$$

$$W = \frac{3.324.943 \cdot 287 \cdot 300}{0{,}4}\left[1 - \left(\frac{1{,}5 \times 10^6}{6{,}0 \times 10^6}\right)^{0{,}286}\right]$$

$$W \approx 715{,}693 \cdot 10^9 \cdot (1 - 0{,}673) \approx 234 \cdot 10^9 \text{ J}$$

Applying Equation (3) the storage of energy (E) can be estimated as:

$$E = \frac{234 \cdot 10^9}{3{,}6 \cdot 10^9} \approx 65 \text{ MWh per cavern}$$

Thus, the theoretical maximum energy recoverable per full discharge cycle of the entire CAES project (three caverns) it can be estimated that as $E_{project}$ = 195 MWh. Under a more conservative assumption the CAES project could provide an energy storage capacity of approximately 150MWh.

To assess the practical usability of the system, the theoretical energy output is adjusted based on typical round-trip efficiencies. Two representative scenarios are considered. In the first case, assuming a conservative efficiency of 50%, which is typical for an older CAES installation, the usable energy is calculated as approximately 75 MWh. In the second scenario, assuming a modern CAES system with thermal integration and an efficiency of 70%, the usable energy becomes 100 MWh. With respect to this data assuming 300 full charge–discharge cycles annually, the corresponding annual energy output of the Monolith CAES is approximately between 22 GWh (50% efficiency) and 30 GWh (70% efficiency).

Finally, the installed capacity of the Monolithi CAES can be estimated at 20-35MW given a discharge duration of 3-4 hours and the usable storage capacity of the project ranging between 75 and 100MWh.

4. ECONOMIC ASSESSMENT AND TECHNOLOGY COMPARISON

For the investment cost estimation of the CAES system in Monolithi, Ioannina, the basis is the cost range found in the international literature, which indicates that the capital expenditure (CAPEX) for compressed air energy storage projects ranges from €100 to €150 per kWh. Given that the total storage capacity of the proposed project is 150 MWh, the total CAPEX ranges between €19,5 million and €29,3 million, depending on the compressor technology, the geological configuration of the underground space, and the system's energy efficiency. In contrast, for the pumped hydro storage project that is under construction in Amfilochia a major energy storage project in Greece—the total investment cost amounts, to €650 million for a storage capacity of 8.000 MWh according to TERNA Energy [20]. This translates to approximately €81,25 per stored kWh. The OPEX of the Monolithi CAES project, based data from [12] can be estimated at approximately €20/MWh, indicating a promising investment opportunity.

The installation of a small or medium-scale CAES energy storage system, such as the one proposed for Monolithi in Ioannina, is particularly advantageous in cases where there is a need for local energy autonomy and improved power quality in peripheral or isolated grids. Such units are ideal for supporting local industrial loads, agricultural grids, or small residential communities, with the capability to provide power during peak demand periods or supply interruptions.

The proposed installation aims to meet local energy demands, especially in areas with increasing penetration of renewable energy sources (RES). The geological suitability of the area, along with the absence of a need for elevation differences or water resources, makes CAES an attractive alternative to pumped hydro storage.

5. DISCUSSION

The results of this study confirm the technical feasibility of implementing a Compressed Air Energy Storage (CAES) system in artificial underground salt caverns at the Monolithi site.While 2D simulations provided a solid initial assessment, the implementation of 3D modeling proved essential in capturing complex spatial interactions between adjacent caverns, more realistic deformation patterns, and surface uplift due to internal pressurization. These phenomena underline the dual role of internal pressure—not only for energy storage but also for mitigating excavation-related deformations—reinforcing the importance of pressurization control in system design and operation.

Importantly, this study builds upon international experience (e.g., Huntorf and McIntosh plants) while adapting the CAES concept to the Greek geological context. To date, halite formations in Greece have not been utilized for subsurface energy storage. The Monolithi salt dome thus emerges as a promising candidate for pilot implementation, potentially setting a precedent for similar projects across Southern Europe.

Nevertheless, it must be emphasized that several simplifications were made in the current design (creep behavior, seasonal thermal fluctuations, etc.). The uncertainty associated with the above should be efficiently addressed by an investigation campaign that will provide all the required information.

6. CONCLUSION

The implementation of three-dimensional (3D) numerical modeling proved essential in accurately evaluating the structural integrity and performance of the proposed CAES system in the Monolithi salt dome. While 2D simulations offered a useful preliminary assessment, the 3D finite element analysis could fully capture the spatial interactions between caverns, the redistribution of stress fields, and the resulting displacements at the ground surface, offering a significant advantage in the overall spatial optimization of the designated caverns. The 3D results highlighted critical phenomena such as uplift due to internal pressurization and stress relief near cavern wall, features that are key to long-term operational safety that cannot be assessed in 2D-models in a sufficient manner.

This study represents a pioneering step for Greece in exploring the application of underground energy storage technologies that are already proven in Central and Northern Europe. The Monolithi site offers a geological opportunity to align national infrastructure development with European Union priorities for clean, decentralized energy systems. As Greece works to meet its commitments under the EU Green Deal and Fit-for-55 targets, modular CAES installations such as the one proposed here could play a vital role in increasing grid resilience, reducing curtailment of renewable sources, and ensuring energy autonomy for peripheral and rural regions.

In this context, the Monolithi CAES project is more than a technical proof of concept; it is a strategic initiative that embodies the transition toward a decarbonized, flexible, and future-ready energy system anchored not only in sound engineering, but also in alignment with European environmental and energy policies.

7. BIBLIOGRAPHY

[1] Adiabatic Compressed Air Energy Storage. (n.d.). www.ease-storage.eu.
[2] Bauer, S. J., Song, B., & Sanborn, B. (2019). Dynamic compressive strength of rock salts. International Journal of Rock Mechanics and Mining Sciences, 113, 112–120. https://doi.org/10.1016/j.ijrmms.2018.11.004.
[3] Caglayan, D. G., Weber, N., Heinrichs, H. U., Linßen, J., Robinius, M., Kukla, P. A., & Stolten, D. (2020). Technical potential of salt caverns for hydrogen storage in Europe. International Journal of Hydrogen Energy, 45(11), 6793–6805. https://doi.org/10.1016/j.ijhydene.2019.12.161.
[4] Chen, H., Cong, T. N., Yang, W., Tan, C., Li, Y., & Ding, Y. (2009). Progress in electrical energy storage system: A critical review. In Progress in Natural Science (Vol. 19, Issue 3, pp. 291–312). Science Press. https://doi.org/10.1016/j.pnsc.2008.07.014.
[5] Davidson, B., Glendenning, I., Harman, R., & Hart, A. (1980). Large-scale electrical energy storage.
[6] Diabatic Compressed Air Energy Storage. (n.d.). www.ease-storage.eu.
[7] European Parliament, C. 371/08. (2020). A comprehensive European approach to energy storage (2019/2189(INI)) (2021/C 371/08).
[8] Kendall Mongird, Vilayanur Viswanathan, Patrick Balducci, Jan Alam, Vanshika Fotedar, Vladimir Koritarov, Boualem Hadjerioua (2020). An Evaluation of Energy Storage Cost and Performance Characteristics. Energies. 13. 3307. doi:10.3390/en13133307.
[9] Kolano, M., Cała, M., & Stopkowicz, A. (2024). Mechanical Properties of Rock Salt from the Kłodawa Salt Dome—A Statistical Analysis of Geomechanical Data. Materials, 17(14). https://doi.org/10.3390/ma17143564.
[10] Kuczyński, S., Skokowski, D., Włodek, T., & Polański, K. (2015). Compressed air energy storage as backup generation capacity combined with wind energy sector in Poland - implementation possibilities. AGH Drilling, Oil, Gas, 32(1), 23. https://doi.org/10.7494/drill.2015.32.1.23.
[11] Marcus N. (2006). Compressed Air Energy Storage (CAES) 10_2006.
[12] Mountrakis, Dimosthenis. (2010). *Geology and Geotectonic Evolution of Greece*. University Studio Press.
[13] Nikolaou, Evangelos (2010, IGME). Update of Groundwater Data in Epirus.
[14] Papanikolaou, Nikolaos. (1978, IGME). Geophysical Reconnaissance Survey for Rock Salt Exploration in the Areas: (a) Monolithi, Ioannina and (b) Karydea, Arta.
[15] Papastavrou, St. (1978, IGME). Report on the 1977 Investigation Activities for the “Rock Salt of Monolithi” Project.
[16] Safaei, H., Keith, D. W., & Hugo, R. J. (2013). Compressed air energy storage (CAES) with compressors distributed at heat loads to enable waste heat utilization. Applied Energy, 103, 165–179. https://doi.org/10.1016/j.apenergy.2012.09.027.
[17] Shabbir Ahmed A, Patrick J. Balducci, A. & Daniel L. Flowers, L. (2023). Technology Strategy Assessment - Compressed Air Energy Storage. https://www.energy.gov/oe/storage-innovations-2030.
[18] Sofianos, Alexandros, & Nomikos, Pavlos. (2008). *Rock Mechanics*. National Technical University of Athens (NTUA).
[19] Succar, S., & Williams, R. H. (2008). Compressed Air Energy Storage: Theory, Resources, And Applications for Wind Power.
[20] Terna-Energy (2025) Amfilochia Pumped Storage. Source: https://www.terna-energy.com/acivities/erga-antlisotamieysis/antlisotamiefsi-amfilochias/ [accessed June 2025].
[21] Vekios, Pavlos. (1979, IGME). *The Rock Salt of Monolithi, Ioannina*.
[22] Vlachopoulos, N., Diederichs, M. S., Marinos, V., & Marinos, P. (2013). Tunnel behavior is associated with the weak Alpine rock masses of the Driskos Twin Tunnel system, Egnatia Odos Highway. Canadian Geotechnical Journal, 50(1), 91–120. https://doi.org/10.1139/cgj-2012-0025.
[23] Wang, T., Yang, C., Wang, H., Ding, S., & Daemen, J. J. K. (2018). Debrining prediction of a salt cavern used for compressed air energy storage. Energy, 147, 464–476. https://doi.org/10.1016/j.energy.2018.01.071.